

Characterization of the N-polar GaN film grown on C-plane sapphire and misoriented C-plane sapphire substrates by MOCVD

Xiaotao Hu(胡小涛), Yimeng Song(宋祎萌), Zhaole Su(苏兆乐), Haiqiang Jia(贾海强), Wenxin Wang(王文新), Yang Jiang(江洋), Yangfeng Li(李阳锋), and Hong Chen(陈弘)

Citation: Chin. Phys. B, 2022, 31 (**3**): 038103. DOI: 10.1088/1674-1056/ac3bad
Journal homepage: http://cpb.iphy.ac.cn; http://iopscience.iop.org/cpb

What follows is a list of articles you may be interested in

Continuous-wave operation of InAs/InP quantum dot tunable external-cavity laser grown by metal-organic chemical vapor deposition

Yan Wang(王岩), Shuai Luo(罗帅), Haiming Ji(季海铭), Di Qu(曲迪), and Yidong Huang(黄翊东)
Chin. Phys. B, 2021, 30 (**1**): 018106. DOI: 10.1088/1674-1056/abcfa4

Mg acceptor activation mechanism and hole transport characteristics in highly Mg-doped AlGaN alloys

Qing-Jun Xu(徐庆君), Shi-Ying Zhang(张士英), Bin Liu(刘斌), Zhen-Hua Li(李振华), Tao Tao(陶涛), Zi-Li Xie(谢自力), Xiang-Qian Xiu(修向前), Dun-Jun Chen(陈敦军), Peng Chen(陈鹏), Ping Han(韩平), Ke Wang(王科), Rong Zhang(张荣), You-Liao Zheng(郑有炓)
Chin. Phys. B, 2020, 29 (**5**): 058103. DOI: 10.1088/1674-1056/ab7e93

Comparison study of GaN films grown on porous andplanar GaN templates

Shan Ding(丁姗), Yue-Wen Li(李悦文), Xiang-Qian Xiu(修向前), Xue-Mei Hua(华雪梅), Zi-Li Xie(谢自力), Tao Tao(陶涛), Peng Chen(陈鹏), Bin Liu(刘斌), Rong Zhang(张荣), You-Dou Zheng(郑有炓)
Chin. Phys. B, 2020, 29 (**3**): 038103. DOI: 10.1088/1674-1056/ab6c48

Dislocation distributions and tilts in Al(Ga)InAs reverse-graded layers grown on misorientated GaAs substrates

Yang He(何洋), Yu-run Sun(孙玉润), Yongming Zhao(赵勇明), Shuzhen Yu(于淑珍), Jianrong Dong(董建荣)
Chin. Phys. B, 2017, 26 (**3**): 038102. DOI: 10.1088/1674-1056/26/3/038102

Nanodots and microwires of ZrO_2 grown on $LaAlO_3$ by photo-assisted metal-organic chemical vapor deposition

Feng Guo(郭峰), Xin-Sheng Wang(汪薪生), Shi-Wei Zhuang(庄仕伟), Guo-Xing Li(李国兴), Bao-Lin Zhang(张宝林), Pen-Chu Chou(周本初)
Chin. Phys. B, 2016, 25 (**2**): 028103. DOI: 10.1088/1674-1056/25/2/028103

RAPID COMMUNICATION

Characterization of the N-polar GaN film grown on C-plane sapphire and misoriented C-plane sapphire substrates by MOCVD

Xiaotao Hu(胡小涛)[1,2], Yimeng Song(宋祎萌)[4], Zhaole Su(苏兆乐)[1,2], Haiqiang Jia(贾海强)[1,2,3], Wenxin Wang(王文新)[1,3], Yang Jiang(江洋)[1,†], Yangfeng Li(李阳锋)[1,‡], and Hong Chen(陈弘)[1,3,5,§]

[1] *Key Laboratory for Renewable Energy, Beijing Key Laboratory for New Energy Materials and Devices, Beijing National Laboratory for Condensed Matter Physics, Institute of Physics, Chinese Academy of Sciences, Beijing* 100190, *China*

[2] *School of Physical Sciences, University of Chinese Academy of Sciences, Beijing* 100049, *China*

[3] *Songshan Lake Materials Laboratory, Dongguan* 523808, *China*

[4] *School of Mathematics and Physics, Beijing Key Laboratory for Magneto-Photoelectrical Composite and Interface Science, University of Science and Technology Beijing, Beijing* 100083, *China*

[5] *College of Materials Science and Opto-Electronic Technology, University of Chinese Academy of Sciences, Beijing* 100049, *China*

(Received 28 September 2021; revised manuscript received 1 November 2021; accepted manuscript online 20 November 2021)

Gallium nitride (GaN) thin film of the nitrogen polarity (N-polar) was grown on C-plane sapphire and misoriented C-plane sapphire substrates respectively by metal-organic chemical vapor deposition (MOCVD). The misorientation angle is off-axis from C-plane toward M-plane of the substrates, and the angle is 2° and 4° respectively. The nitrogen polarity was confirmed by examining the images of the scanning electron microscope before and after the wet etching in potassium hydroxide (KOH) solution. The morphology was studied by the optical microscope and atomic force microscope. The crystalline quality was characterized by the x-ray diffraction. The lateral coherence length, the tilt angle, the vertical coherence length, and the vertical lattice-strain were acquired using the pseudo-Voigt function to fit the x-ray diffraction curves and then calculating with four empirical formulae. The lateral coherence length increases with the misorientation angle, because higher step density and shorter distance between adjacent steps can lead to larger lateral coherence length. The tilt angle increases with the misorientation angle, which means that the misoriented substrate can degrade the identity of crystal orientation of the N-polar GaN film. The vertical lattice-strain decreases with the misorientation angle. The vertical coherence length does not change a lot as the misorientation angle increases and this value of all samples is close to the nominal thickness of the N-polar GaN layer. This study helps to understand the influence of the misorientation angle of misoriented C-plane sapphire on the morphology, the crystalline quality, and the microstructure of N-polar GaN films.

Keywords: metal-organic chemical vapor deposition (MOCVD), misoriented sapphire substrate, misorientation angle, x-ray diffraction, N-polar GaN

PACS: 81.05.Ea, 81.20.Ka, 87.64.Bx, 87.64.Aa **DOI:** 10.1088/1674-1056/ac3bad

1. Introduction

Gallium nitride (GaN) is a fundamental semiconductor material that has been applied to light emitting diodes (LEDs),[1] laser diodes (LDs),[2] as well as high electron mobility transistors (HEMTs),[3] etc. Normally, GaN has a crystal structure of wurtzite, with C-plane (0001) as basal plane. Meanwhile, C-plane is a polar plane and it can exhibit two kinds of polarities, the Ga-polar (0001) and the N-polar ($000\bar{1}$). The Ga-polar is the common polarity, and the Ga-polar GaN film can be grown by the metal-organic chemical vapor deposition (MOCVD) or the molecular beam epitaxy (MBE) on the sapphire (0001), Si (111), or the SiC substrates.[4–11] And the growth and the application of Ga-polar GaN have been studied extensively and deeply.[6,11–17] On the other hand, the N-polar is the rare polarity, and the N-polar GaN film has many advantages over the Ga-polar GaN film. For example, in the N-polar AlGaN/GaN HEMT, GaN channel layer is on the top of AlGaN barrier layer. Such structure leads to lower resistance of Ohmic contact and less electron scattering in the channel compared with the Ga-polar AlGaN/GaN HEMT. Besides, the N-polar GaN is easier to be manufactured into the enhancement mode transistors and the N-polar HEMTs have the advantage over Ga-polar HEMTs when they are scaled down.[18] Nevertheless, a high density of hexagonal hillocks appeared on the surface of the N-polar GaN layer grown on the C-plane sapphire by MOCVD.[19] The N-polar GaN without the hexagonal hillocks on the surface was grown by Matsuoka *et al.*[20] on the C-plane sapphire by MOCVD and it showed the surface and a small full width at half maximum (FWHM) of the x-ray rocking curves for the ($000\bar{2}$) reflection. Keller *et al.*[21] also grew the N-polar GaN without the hexagonal hillocks by MOCVD on the misoriented sapphire substrate, for the possible mechanism that the misori-

†Corresponding author. E-mail: jiangyang@iphy.ac.cn
‡Corresponding author. E-mail: liyangfeng12@mails.ucas.ac.cn
§Corresponding author. E-mail: hchen@iphy.ac.cn

© 2022 Chinese Physical Society and IOP Publishing Ltd

ented sapphire offered more steps and kinks that can promote the step flow growth. Nowadays, the crystalline quality and surface morphology of the N-polar GaN have been greatly improved, but the growth window is narrower than that of the Ga-polar GaN, because the growth mechanism, the crystal defects and the microstructure of the N-polar GaN are still lack of deep understanding.

X-ray diffraction (XRD) is an important tool in characterizing the thin film. The diffraction curves can be fitted by the Gaussian distribution function or the Lorentzian distribution function or more complex functions, like the Voigt,[22] the pseudo-Voigt[23] and the Pearson,[24] and these complex functions can approach the curve closer than the Gaussian function or Lorentzian function.[22] The mathematic form of the pseudo-Voigt function is a linear combination of Gaussian function and Lorentzian function,[24] and it is simpler than the form of the other two complex functions, so in this study we pick it as the fitting function. It is known[23,25] that in the ω–2θ scan for XRD, the Gaussian distribution function is only related to the vertical lattice-strain in the film, and the Lorentzian distribution function is only related to the vertical coherence length in the film. And in the ω scan for XRD, the Gaussian function is only related to the tilt angle of crystallites in the film and the Lorentzian function is only related to the lateral coherence length in the film. Therefore, the contributions of the vertical lattice-strain and the vertical coherence length to the diffraction curve can be separated and the values of these two parameters can be calculated. Similarly, the tilt angle and the lateral coherence length can be calculated.

In this paper, the N-polar GaN film was grown on the C-plane sapphire and misoriented C-plane sapphire substrates respectively by MOCVD. The polarity of the film was testified and the morphology was studied. More importantly, the contributions of the vertical lattice-strain and the vertical coherence length and the contributions of the tilt angle and the lateral coherence length to the diffraction curve were separated respectively, and the influence of different misorientation angles on these parameters was investigated.

2. Experiment

The N-polar GaN film was grown on three sapphire substrates in one run by the AIXTRON G3[26] 2400HT MOCVD. The three substrates were C-plane sapphire, C-plane sapphire with 2° off-axis toward M-plane, and C-plane sapphire with 4° off-axis toward M-plane. All the substrates were two inches in diameter and 430-μm-thick. The precursors were trimethylgallium (TMGa), trimethyl-aluminum (TMAl) and ammonia (NH_3). The growth consisted of four steps. Firstly, the three substrates were kept at 1000 °C for 20 min in an atmosphere of H_2 to desorb molecules on the surface. Next, a 3-min nitridation occurred at 1000 °C in an atmosphere of NH_3. Then, a 100-nm-thick AlN nucleation layer was grown. Lastly, the N-polar GaN layer was grown at 1050 °C. The nominal thickness of the N-polar GaN layer was 1 μm. The reactor pressure was kept constant at 50 mbar during the growth. The three as-grown samples were named as sample 0M, sample 2M, and sample 4M, where 0M, 2M and 4M represent the N-polar GaN film grown on the C-plane sapphire, on the C-plane sapphire with 2° off-axis toward M-plane and on the C-plane sapphire with 4° off-axis toward M-plane, respectively. To confirm the polarity of the as-grown films, we adopt the method of wet etching. The samples were first immersed in potassium hydroxide (KOH) solution (6 mol/L) at room temperature for 5 min, and then were observed under the scanning electron microscope (SEM, SIRION FP6800/73).

The XRD curves were recorded by the x-ray diffractometer (Malvern Panalytical EMPYREAN), using a wavelength of 1.540598 Å (Cu $K_{\alpha 1}$). The reflection geometry includes a Ge (220) hybrid monochromator and a hybrid pixel detector (PIXcel 3D). The surface morphology of the as-grown samples was examined by the optical microscope (OM, Nikon ECLIPSE LV15ON) and atomic force microscope (AFM, Bruker MultiMode 8, in ScanAsyst Mode).

To acquire the lateral coherence length and the tilt angle (the "lateral" means the direction is parallel to the surface of the film), we used the pseudo-Voigt function to fit the measured $(000\bar{2})$ ω-scan curve, and the pseudo-Voigt function is[23]

$$P(x) = I_0\left[\eta L(x) + (1-\eta)\,G(x)\right],\ \ 0 \leqslant \eta \leqslant 1, \tag{1}$$

where $L(x)$ and $G(x)$ are the Lorentzian distribution function and the Gaussian distribution function, respectively, η is the variable of the pseudo-Voigt function, and I_0 is a scaling constant. The lateral coherence length and the tilt angle were calculated using the following empirical formulae:[23]

$$L_{\parallel} = \frac{0.9\lambda}{\beta_\omega\left(0.017475+1.500484\eta-0.534156\eta^2\right)\sin\theta}, \tag{2}$$

$$\alpha = \beta_\omega[0.184446+0.812692\,(1-0.998497\eta)^{1/2} -0.659603\eta+0.44554\eta^2], \tag{3}$$

where λ is the x-ray wavelength, θ is the Bragg angle for the $(000\bar{2})$ reflection, and β_ω is the integral breadth of the fitting curve.

To acquire the vertical coherence length and the vertical lattice-strain (the "vertical" means the direction is normal to the surface of the film), we used the pseudo-Voigt function to fit the $(000\bar{2})$ ω–2θ scan curve. And the vertical coherence length and the vertical lattice-strain were calculated using the following empirical formulae, respectively:[23]

$$L_{\perp} = \frac{0.9\lambda}{\beta_{2\theta-\theta}\left(0.017475+1.500484\eta-0.534156\eta^2\right)\cos\theta}, \tag{4}$$

$$e_{\perp} = \frac{1}{4\tan(\theta)}\beta_{2\theta-\theta}\left[0.184446 + 0.812692\,(1-0.998497\eta)^{\frac{1}{2}} - 0.659603\eta + 0.445542\eta^{2}\right], \quad (5)$$

where $\beta_{2\theta-\theta}$ is the integral breadth of the fitting curve, and θ is the Bragg angle for the $(000\bar{2})$ reflection.

3. Results and discussion

Figure 1 shows the SEM photographs of the samples before and after KOH etching. Before the etching, a hexagonal hillock is on the surface of sample 0M. After the etching, a hexagonal hillock can still be seen and many little hillocks appear on the surface, as shown in Figs. 1(a) and 1(b). These small hillocks are hexagonal too (the relevant photographs are given in Appendix A). As shown in Figs. 1(c) and 1(d), before the etching, an irregular hexagonal hillock is on the surface of sample 2M, and many small hillocks also appear on the surface after the etching. Figure 1(e) shows the surface of sample 4M before KOH etching and some tortuous wrinkles can be seen on the surface. After KOH etching, as shown in Fig. 1(f), the wrinkles are gone, and the surface is covered with many little hillocks. According to Ng, Weimann and Chowdhury,[27] Ga-polar GaN film remained intact in the KOH solution while N-polar film was etched in the solution and later on the surface was covered with many nanotip pyramids, which are consistent with the small hillocks in Figs. 1(b), 1(d), and 1(f). Therefore, it is confirmed that the three samples are all N-polar GaN thin films.

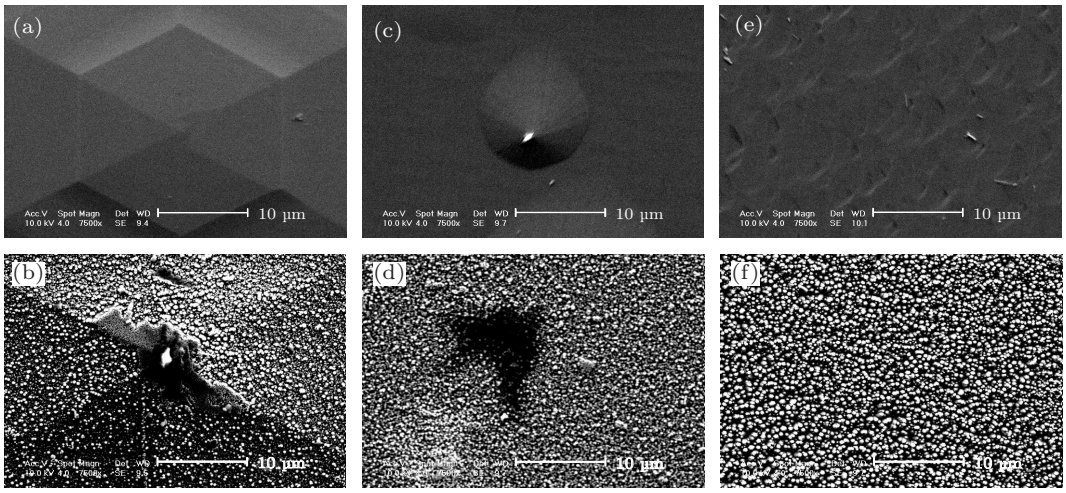


Fig. 1. Plane-view SEM photographs of the as-grown samples ((a), (c), (e)) and the samples after KOH etching ((b), (d), (f)). (a), (b) sample 0M; (c), (d) sample 2M; and (e), (f) sample 4M. The accelerate voltage, the spot size, and the magnification are all the same for these photographs.

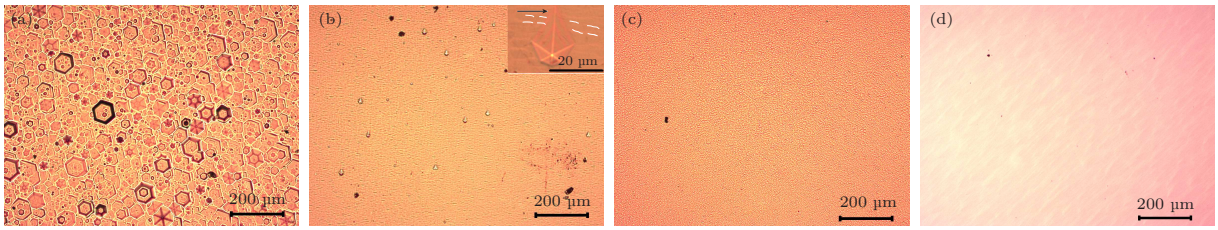


Fig. 2. The plane-view optical micrographs of (a)–(d) samples 0M, 2M, 4M and a Ga-polar sample, respectively.

Figure 2 shows the photographs of the surface of N-polar GaN samples and a Ga-polar GaN sample taken by the optical microscope. Many hexagonal hillocks are on the surface of sample 0M, as shown in Fig. 2(a). In Fig. 2(b), a small number of hillocks are on the surface of sample 2M, and their sizes are smaller than those on the surface of sample 0M. An insert in Fig. 2(b) shows an enlarged hillock, and we can see that the shape of the hillock is an irregular hexagon. The wrinkles on the surface, which are indicated by two broken white lines, can be clearly recognized. The sharpest corner in the insert indicated by a black arrow represents the fastest growth direction of the hillock, and this corner is perpendicular to the wrinkles on the surface. No hillocks appear on the surface of sample 4M, as shown in Fig. 2(c), and the surface is very smooth. Keller *et al.*[21] have reported similar results. What's more, our results show that the shape of the hillocks on sample 2M is irregular and all the hillocks' sharpest corner is parallel to the misorientation direction of the sapphire substrate. We believe that the irregular shape of the hexagonal hillocks is caused by the misoriented substrate. From sample 2M to 4M, the density of hillocks can drop to zero. The explanation is that increasing the misorientation angle leads to the increase of the step

density on the surface of the sapphire substrate, and adatoms can combine with each other more easily because of the decreased distance between adjacent steps. Therefore, they are more likely to coalesce into one complete film. Finally, the Ga-polar GaN sample exhibits a smooth surface, as shown in Fig. 2(d), and this sample is grown on the C-plane sapphire substrate. The difference of Ga-polar and N-polar GaN is that it is easy to get Ga-polar GaN film with a smooth surface on C-plane sapphire substrate, while smooth N-polar GaN film can only appear on misoriented substrate with a proper misorientation angle.

The root-mean-square roughness of samples 0M, 2M and 4M is 5.19 nm, 2.64 nm and 5.26 nm, respectively. Of the three samples, sample 2M has the lowest roughness. And the morphology of samples 2M and 4M is different from that of sample 0M. As shown in Figs. 3(b) and 3(c), small undulations with peaks and valleys[21] can be clearly seen on the surfaces of samples 2M and 4M, while a hillock-like morphology can be seen on the surface of sample 0M in Fig. 3(a). The undulations of samples 2M and 4M are probably due to the step bunching.[21] In general, the morphology of the N-polar GaN changes from hillocks on the C-plane sapphire to the undulations with peaks and valleys on the misoriented sapphire.

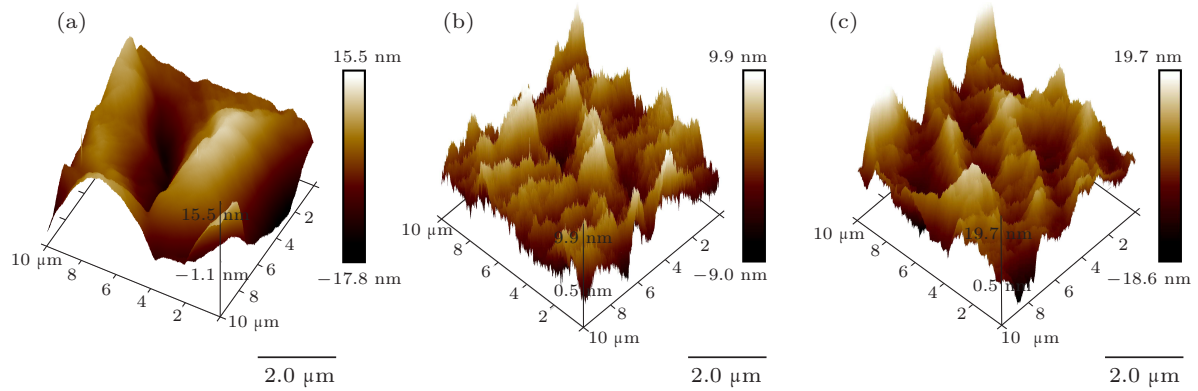


Fig. 3. (a)–(c) The AFM images of the surfaces of samples 0M, 2M and 4M, respectively. The scanning area is 10×10 μm^2.

Figure 4 shows the FWHM of $(000\bar{2})$ and $(10\bar{1}\bar{2})$ of the samples for the x-ray rocking curves. With the increase of the substrate misorientation angle, the FWHM of $(10\bar{1}\bar{2})$ is greatly improved (from 770 arcsec to 450 arcsec), while the FWHM of $(000\bar{2})$ shows a modest increase especially when the misorientation angle is not too large. The result implies that further increase of the misorientation angle of the sapphire substrate probably leads to the deterioration of crystal quality of the GaN film. In general, the crystalline quality of the N-polar GaN film is improved by introducing the substrate misorientation.

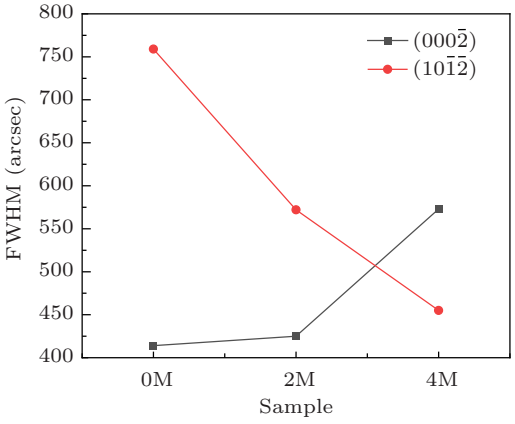


Fig. 4. The FWHM of $(000\bar{2})$ and $(10\bar{1}\bar{2})$ of the three samples for the x-ray rocking curves, with the symbol squares and circles representing the FWHM of $(000\bar{2})$ and $(10\bar{1}\bar{2})$, respectively.

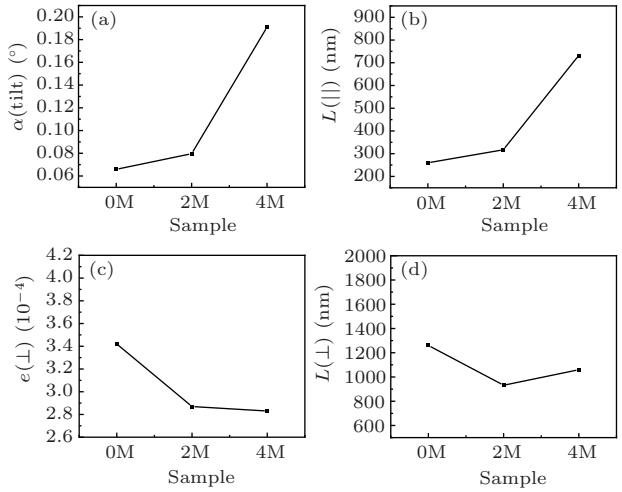


Fig. 5. The calculated (a) tilt angle, (b) lateral coherence length, (c) vertical lattice-strain, (d) vertical coherence length of the three samples from the pseudo-Voigt function fit.

As shown in Fig. 5(a), from sample 0M to 2M and then to 4M, the tilt angle increases. This means that the crystallites deviate more from the $[000\bar{1}]$ orientation when growing on the misoriented substrate, so the crystal orientation of the N-polar GaN film is degraded. This situation gets worse when the misorientation angle increases. The lateral coherence length increases too, as shown in Fig. 5(b). The explanation is that the substrate of sample 4M contains higher density of steps on the surface than those of 2M and 0M do. During the growth, the

adatoms at the steps of sample 4M's surface only need to diffuse a short distance to the adjacent step to combine with other adatoms to form a crystallite, and hence the crystallites have larger lateral length. As shown in Fig. 5(c), from sample 0M to 2M and then to 4M, the vertical lattice-strain decreases. Furthermore, from sample 0M to 2M, the decrease of the lattice-strain is significant, while from sample 2M to 4M, it is much less. It means that the misorientation angle has limited effect on the decrease of the vertical lattice-strain. The vertical coherence lengths of samples 0M, 2M and 4M do not show much difference, as shown in Fig. 5(d), and the lengths of the three samples are all close to 1 μm, which is the nominal thickness of the samples, and this result is similar to that of the Ga-polar GaN film.[23]

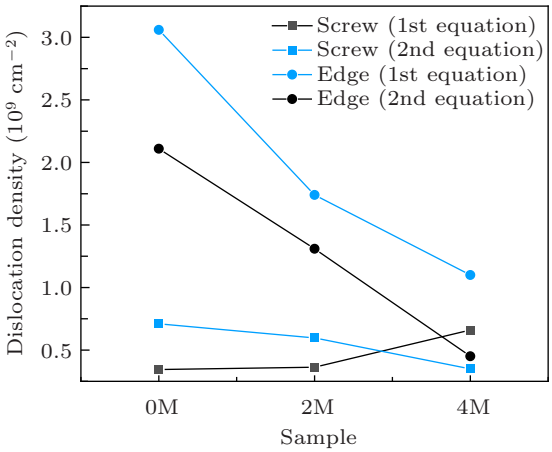


Fig. 6. The calculated screw and edge dislocation density of samples 0M, 2M and 4M.

It is known that the FWHM of $(000\bar{2})$ of XRD can be used to calculate the density of the screw threading dislocations ($\boldsymbol{b} = \langle 0001 \rangle$, $|\boldsymbol{b}| = 0.5185$ nm), and the FWHM of $(10\bar{1}\bar{2})$ of XRD can be used to calculate the density of the edge threading dislocations ($\boldsymbol{b} = 1/3\langle 11\bar{2}0 \rangle$, $|\boldsymbol{b}| = 0.3189$ nm).[21] The dislocation density is overestimated because the mixed dislocation ($\boldsymbol{b} = 1/3\langle 11\bar{2}3 \rangle$) can contribute to FWHM of both reflections. To calculate the density of dislocation, we use two different equations. The first one is $N = \beta^2/(4.35 \cdot b^2)$, and the second one is $N = \beta/(2.1 \cdot b \cdot d_0)$, β is the FWHM of the x-ray rocking curves, $\boldsymbol{b}$ is the magnitude of the burgers vector, and d_0 in the second equation is the spacing between subgrain boundary according to Dunn and Koch.[28] The difference between the two equations is that the first one assumes that the dislocations are randomly distributed in the film, while the second assumes that the dislocations only locate at the boundary of subgrains. In this case, we can consider the mosaic blocks as the subgrains and use the lateral coherence length to replace the d_0. The results are given in Fig. 6. An interesting phenomenon can be seen, that is, the screw dislocation density of sample 4M calculated from the first equation is the largest among the three samples, while from the second equation it is the smallest. On the contrary, the screw dislocation density of sample 0M calculated from the first equation is the smallest, while from the second equation it is the largest. The edge dislocation density of each sample calculated from the first equation is larger than that calculated from the second equation.

4. Conclusion

The N-polar GaN films were grown on the C-plane sapphire substrate, the C-plane sapphire with 2° off-axis toward M-plane and the C-plane sapphire with 4° off-axis toward M-plane by MOCVD. The polarity was testified by the KOH solution etching and the SEM observation. The density of the hexagonal hillocks on the surface of the samples drops as the misorientation angle increases. The crystalline quality of samples 2M and 4M is better than that of sample 0M, and sample 2M has lower RMS roughness than samples 0M and 4M. However, a small density of irregular hexagonal hillocks still appears on the surface of sample 2M, which is a problem that needs to fix in the future. The increase of the misorientation angle can enlarge the tilt angle and the lateral coherence length of the crystallites. What's more, the increase of the misorientation angle can lower the vertical lattice-strain, but do not influence much on the vertical coherence length. This study helps to understand the influence of the misorientation angle of the misoriented C-plane sapphire on the morphology, the crystalline quality and the microstructure of the N-polar GaN film.

Acknowledgements

This work was supported by the National Natural Science Foundation of China (Grant No. 61991441), the Strategic Priority Research Program of Chinese Academy of Sciences (Grant No. XDB33000000), and Youth Innovation Promotion Association of Chinese Academy of Sciences. We thank Yang X A from the Advanced Materials Laboratory, Institute of Physics, Chinese Academy of Sciences, for the experimental work of scanning electron microscope (SEM Sirion).

References

[1] Roccato N, Piva F, Santi C D, Brescancin R, Mukherjee K, Buffolo M, Haller C, Carlin J F, Grandjean N, Vallone M, Tibaldi A, Bertazzi F, Goano M, Verzellesi G, Meneghesso G, Zanoni E and Meneghini M 2021 *J. Phys. D: Appl. Phys.* **54** 425105
[2] Ide T, Iida R, Takeuchi T, Wang X L, Takada N and Shimizu M 2021 *Jpn. J. Appl. Phys.* **60** SBBE01
[3] Pągowska K, Kozubal M, Taube A, Kruszka R, Kamiński M, Kwietniewski N, Juchniewicz M and Szerling A 2021 *Mater. Sci. Semicond. Process.* **127** 105694
[4] Johnson M A L, Fujita S, Rowland W H, Hughes W C, He Y W, El-Masry N A, Cook J W, Schetzina J F, Ren J and Edmond J A 1996 *J. Electron. Mater.* **25** 793
[5] Shen X Q, Okumura H, Furuta K and Nakamura N 2006 *Appl. Phys. Lett.* **89** 171906
[6] Kuo D H and Wu W H 2009 *Chem. Vap. Depos.* **15** 11
[7] Wang Y, Hu F and Hane K 2011 *Nanoscale Res. Lett.* **6** 117
[8] Zhang J, Li S, Xiong H, Tian W, Li Y, Fang Y, Wu Z, Dai J, Xu J, Li X and Chen C 2014 *Nanoscale Res. Lett.* **9** 1

[9] Chen Y, Song H, Li D, Sun X, Jiang H, Li Z, Miao G, Zhang Z and Zhou Y 2014 *Mater. Lett.* **114** 26

[10] Feng Y, Wei H, Yang S, Zhang H, Kong S, Zhao G and Liu X 2014 *CrystEngComm* **16** 7525

[11] Kadys A, Malinauskas T, Grinys T, Dmukauskas M, Mickevičius J, Aleknavičius J, Tomašiūnas R, Selskis A, Kondrotas R, Stanionytė S, Lugauer H and Strassburg M 2015 *J. Electron. Mater.* **44** 188

[12] Nakamura S, Senoh M and Mukai T 1993 *Jpn. J. Appl. Phys.* **32** L8

[13] Asif Khan M, Bhattarai A, Kuznia J N and Olson D T 1993 *Appl. Phys. Lett.* **63** 1214

[14] Nakamura S, Masayuki S, Nagahama S, Iwasa N, Yamada T, Matsushita T, Kiyoku H and Sugimoto Y 1996 *Jpn. J. Appl. Phys.* **35** L74

[15] Song Y, He Y, Li Y, Wei H, Qiu P, Huang Q, He Z, Die J, Peng M and Zheng X 2021 *Cryst. Growth Des.* **21** 1778

[16] Li Y, Deng Z, Ma Z, Wang L, Jia H, Wang W, Jiang Y and Chen H 2019 *J. Appl. Phys.* **126** 095705

[17] Li Y, Yan S, Hu X, Song Y, Deng Z, Du C, Wang W, Ma Z, Wang L, Jia H, Wang W, Zhou J, Jiang Y and Chen H 2020 *Superlattices Microstruct.* **145** 106606

[18] Wong M H and Mishra U K 2019 *Semiconductors and Semimetals* **102** 329

[19] Rouviére J L, Arlery M, Niebuhr R, Bachem K H and Briot O 1997 *Mater. Sci. Eng. B* **43** 161

[20] Matsuoka T, Kobayashi Y, Takahata H, Mitate T, Mizuno S, Sasaki A, Yoshimoto M, Ohnishi T and Sumiya M 2006 *Phys. Status Solidi Basic Res.* **243** 1446

[21] Keller S, Fichtenbaum N A, Wu F, Brown D, Rosales A, Denbaars S P, Speck J S and Mishra U K 2007 *J. Appl. Phys.* **102** 083546

[22] de Keijser T H, Langford J I, Mittemeijer E J and Vogels A B P 1982 *J. Appl. Crystallogr.* **15** 308

[23] Metzger T, Höpler R, Born E, Ambacher O, Stutzmann M, Stömmer R, Schuster M, Göbel H, Christiansen S, Albrecht M and Strunk H P 1998 *Philos. Mag. A Phys. Condens. Matter, Struct. Defects Mech. Prop.* **77** 1013

[24] de Keijser T, Mittemeijer E J and Rozendaal H C F 1983 *J. Appl. Crystallogr.* **16** 309

[25] Chierchia R, Böttcher T, Heinke H, Einfeldt S, Figge S and Hommel D 2003 *J. Appl. Phys.* **93** 8918

[26] Beccard R, Protzmann H, Schmitz D A, Strauch G, Heuken M and Juergensen H 1998 *Proc. SPIE, Optoelectronic Materials and Devices* **3419** 70

[27] Ng H M, Weimann N G and Chowdhury A 2003 *J. Appl. Phys.* **94** 650

[28] Dunn C G and Koch E F 1957 *Acta Metallurgica* **5** 548